

## Drastic Modulation of Stimuli-Responsive Fluorescence by Subtle Structural Change of Organic Fluorophore and Polymorphism Controlled Mechanofluorochromism

Palamarneri Sivaraman Hariharan, gayathri parthasarathy, Anu Kundu, Subramanian Karthikeyan, Yoshimitsu Sagara, Dohyun Moon, and Savarimuthu Philip Anthony

*Cryst. Growth Des.*, **Just Accepted Manuscript** • DOI: 10.1021/acs.cgd.8b00310 • Publication Date (Web): 24 May 2018

Downloaded from <http://pubs.acs.org> on May 24, 2018

### Just Accepted

“Just Accepted” manuscripts have been peer-reviewed and accepted for publication. They are posted online prior to technical editing, formatting for publication and author proofing. The American Chemical Society provides “Just Accepted” as a service to the research community to expedite the dissemination of scientific material as soon as possible after acceptance. “Just Accepted” manuscripts appear in full in PDF format accompanied by an HTML abstract. “Just Accepted” manuscripts have been fully peer reviewed, but should not be considered the official version of record. They are citable by the Digital Object Identifier (DOI®). “Just Accepted” is an optional service offered to authors. Therefore, the “Just Accepted” Web site may not include all articles that will be published in the journal. After a manuscript is technically edited and formatted, it will be removed from the “Just Accepted” Web site and published as an ASAP article. Note that technical editing may introduce minor changes to the manuscript text and/or graphics which could affect content, and all legal disclaimers and ethical guidelines that apply to the journal pertain. ACS cannot be held responsible for errors or consequences arising from the use of information contained in these “Just Accepted” manuscripts.



## Drastic Modulation of Stimuli-Responsive Fluorescence by Subtle Structural Change of Organic Fluorophore and Polymorphism Controlled Mechanofluorochromism

Palamarneri Sivaraman Hariharan,<sup>a</sup> Parthasarathy Gayathri,<sup>a</sup> Anu Kundu,<sup>a</sup> Subramanian Karthikeyan,<sup>b</sup> Yoshimitsu Sagara<sup>c</sup> Dohyun Moon<sup>d\*</sup> Savarimuthu Philip Anthony<sup>a\*</sup>

<sup>a</sup>School of Chemical & Biotechnology, SASTRA Deemed University, Thanjavur-613401, Tamil Nadu, India. Fax: +914362264120; Tel: +914362264101; E-mail: philip@biotech.sastra.edu

<sup>b</sup>PG and Research department of chemistry, Khadir Mohideen College, Adirampattinam, Tamil Nadu, India.

<sup>c</sup>Research Institute for Electronic Science, Hokkaido University, N20, W10, Kita-Ku, Sapporo 001-0020, Japan

<sup>d</sup>Beamline Department, Pohang Accelerator Laboratory, 80 Jigokro-127beongil, Nam-gu, Pohang, Gyeongbuk, Korea, Email: dmoon@postech.ac.kr

**KEYWORDS.** Smart fluorescent materials, fluorescence switching, polymorphism, fluorescence tuning, topochemical conversion

**ABSTRACT:** Stimuli-responsive fluorescence modulation of organic fluorophores is closely related to their structural organization, non-covalent interactions, ability to adopt different conformation and phase change in the solid state. Herein, we have synthesized aggregation enhanced emissive (AEE) fluorophores, (5-(4-(diphenylamino)benzylidene)-2,2-dimethyl-1,3-dioxane-4,6-dione (**1**), 5-(4-(diphenylamino)-2-methoxybenzylidene)-2,2-dimethyl-1,3-dioxane-4,6-dione (**2**) and 5-(4-(diphenylamino)-4-methoxybenzylidene)-2,2-dimethyl-1,3-dioxane-4,6-dione (**3**)) and demonstrated molecular structure controlled tunable fluorescence (552 to 616 nm,  $\Phi_f = 14.6\text{--}41.8\%$ ) and stimuli-responses. **1** showed thermofluorochromism (TFC) between 586 and 558 nm at room and lig.N<sub>2</sub>. **2** showed tunable fluorescence via polymorphism (**2a** (550 nm) and **2b** (610 nm)). Interestingly, hard crushed - **2b** polymorph showed two different MFC when heated at 80 and 180 °C as well as topochemical conversion from **2b** to **2a**. In contrast, **2a** and **3** displayed usual mechanofluorochromism (MFC). Crystal structure, powder X-ray diffraction (PXRD) and differential scanning calorimetric (DSC) studies indicated conformational, structural and phase change at different stimuli and responsible for fluorescence switching/tuning. Computational studies revealed optical band gap modulation depend on the molecular conformation and support the fluorescence modulation.

### 1. Introduction

The ability of organic fluorophores to exhibit tunable and switchable solid state fluorescence have attracted considerable attention because of their application in optical switches, organic light-emitting diodes (OLEDs), data recording, sensors, displays, photo dynamic therapy and bio-imaging.<sup>1-12</sup> Particularly, smart fluorescent materials that responds systematic modulation to the external stimuli such as pressure, heat, vapor and pH are highly desirable since that can bring new functional adaptive properties. Molecular conformation, packing and non-covalent interaction strongly influenced on the solid state fluorescence.<sup>13-22</sup> Fundamental interest and application potential in optoelectronic devices lead to the development of large number of MFC and thermofluorochromic (TFC) derivatives including imidazoles.<sup>23-42</sup> Most of the reported MFC and TFC materials showed fluorescence color change between two emissive or one emissive and one non-emissive state; though multi-color emitting MFC and TFC materials have also been reported.<sup>43-46</sup> Mechanical forces convert the fluorescence color via modulating molecular conformation/non-covalent interaction/phase of the materials and produce meta-stable state whereas heating or vapor exposure recovered the initial fluo-

rescence.<sup>38</sup> Some of the MFC materials have also showed self-reversible gradual change of fluorescence with mechanical force.<sup>47-48</sup> Self-reversible and switchable fluorescence has been reported for TFC materials by controlling rate of heating and cooling.<sup>49-51</sup> Mechano and thermo-responsive supramolecular polymer and unique MFC at higher temperature has also been recently reported.<sup>52,53</sup> Polymorphism provided opportunity to develop tunable organic fluorescent materials without altering chemical structure.<sup>54-60</sup> Tunable fluorescence by topochemical conversion, transforming one polymorph to another by thermal treatment and mechanical force, has also been realized.<sup>38,54,61</sup> However, modulation of stimuli-response by subtle structural change, especially polymorphic structure exhibiting different MFC depends on the heating temperature and gradual fluorescence change from one polymorph to another remains scarcely explored.

Triphenylamine (TPA) has often been employed for developing organic materials for dye sensitized solar cell, organic light emitting diode (OLED), field effect transistor, sensor, solid state fluorescent and smart fluorescent materials by utilizing non-planar propeller shape, synthetic tailorability and good optoelectronic.<sup>62-66</sup> The conformational robustness and propeller core of TPA hindered close packing of fluorophore

in the solid state that produced AEE and MFC.<sup>67-69</sup> Self-reversible and reversible MFC, tunable solid state fluorescence via polymorphism, self-erasable and rewritable fluorescent platforms have been demonstrated using TPA by tailoring acceptor structure, substituent position and halochromic functionality.<sup>28-32</sup> In this manuscript, we have synthesized three new fluorophores (**1-3**) based on TPA donor and meldrum's acid acceptor (Scheme 1) that exhibited molecular structure controlled reversible TFC, polymorphs controlled MFC, topochemical conversion and usual MFC. **1-3** showed tunable strong fluorescence in the solid state (552 to 616 nm,  $\Phi_f = 14.6-41.8\%$ ). **1** exhibited reversible fluorescence switching between 586 and 558 nm at room temperature and liq. N<sub>2</sub>, respectively. **2** produced polymorphism induced tunable fluorescence (**2a** (553 nm) and **2b** (610 nm)). **2a** displayed usual MFC while applying mechanical force and heating. In contrast, **2b** exhibited two different MFC when heated at 80 and 180 °C as well as topochemical conversion from **2b** to **2a**. Hard crushing of **2b** showed blue shift of fluorescence (577 nm) with substantial reduction of intensity. Interestingly, heating at 80 °C exhibited turn-on fluorescence at 607 nm (**2b**) whereas 180 °C heating converted **2b** to **2a** and showed fluorescence at 550 nm. **3** showed usual off-on fluorescence switching. Crystal structure analysis of **1** at different temperature revealed slight molecular conformational change without packing modulation. PXRD pattern also showed slight variation in the peak position at different temperature. The polymorphs of **2** exhibited distinctly different conformation and molecular organization in the crystals. PXRD studies of **2b** showed clear change of structure from **2b** to **2a** with increasing heating temperature. DSC analysis and computational studies further provided insight on the fluorescence change. Thus the present studies demonstrated structure controlled stimuli-responses and rare polymorphism controlled MFC in a organic fluorophore.

## 2. Experimental Section

Triphenylamine, 3-methoxy-N,N-diphenylaniline, 4-methoxy triphenylamine, dimethylformamide (DMF, HPLC grade), phosphorous oxychloride and 2,2'-dimethyl-1,3-dioxane-4,6-dione were purchased from Sigma-Aldrich and used without further purification. Aldehyde functional group into triphenylamine, 3-methoxy triphenylamine and 4-methoxy triphenylamine was introduced by following reported procedure.<sup>70</sup>

### General procedure for synthesizing **1-3** (Scheme S1)

To the stirred solution of aldehyde (4-(diphenylamino)benzaldehyde/4-(diphenylamino)-2-methoxybenzaldehyde/4-((4-methoxyphenyl)(phenyl)amino)benzaldehyde) (1.0 equivalent) in methanol, 1.1 equivalents of 2,2'-dimethyl-1,3-dioxane-4,6-dione was added and stirred at room temperature for 6 hrs. The precipitated product from the reaction mixture was filtered and washed with cold methanol and dried.

#### 1

Orange crystalline powder. Yield: 85%. M. p.: 190 °C, <sup>1</sup>H-NMR (300 MHz, CDCl<sub>3</sub>) δ 8.43 (s, 1H), 8.23 (d, 2H), 7.39-7.34 (m, 4H), 7.26-7.19 (m, 6H), 6.94 (d, 2H), 3.41 (s, 3H), 3.38 (s, 3H). <sup>13</sup>C-NMR (75 MHz, CDCl<sub>3</sub>) δ 163.56, 161.27, 158.37, 153.16, 151.61, 145.43, 138.05, 129.82, 126.73, 125.81, 124.55, 117.92, 112.25, 29.00, 28.31. C<sub>25</sub>H<sub>21</sub>NO<sub>4</sub>

(399.44): calcd. C 75.17, H 5.30, N 3.51; found C 75.44, H 5.64, N 3.62. LCMS (ESI) calcd. [M<sup>+</sup>]: 399.15, found: 399.2.

#### 2

Bright orange crystalline powder. Yield: 80%. M. p.: 227 °C, <sup>1</sup>H-NMR (300 MHz, CDCl<sub>3</sub>) δ 8.87 (s, 1H), 8.43 (d, 1H), 7.40-7.35 (m, 4H), 7.25-7.20 (m, 6H), 6.49 (dd, 1H), 6.34 (d, 1H), 3.68 (s, 3H), 1.76 (s, 6H). <sup>13</sup>C-NMR (75 MHz, CDCl<sub>3</sub>) δ 164.9, 163.0, 161.4, 155.7, 151.4, 145.3, 135.4, 129.8, 126.9, 126.0, 113.8, 111.3, 107.1, 103.6, 99.8, 55.6, 27.4. C<sub>26</sub>H<sub>23</sub>NO<sub>5</sub> (429.46): calcd. C 72.71, H 5.40, N 3.26; found C 72.56, H 5.56, N 3.12. LCMS (ESI) calcd. [M<sup>+</sup>]: 429.16, found: 429.2.

#### 3

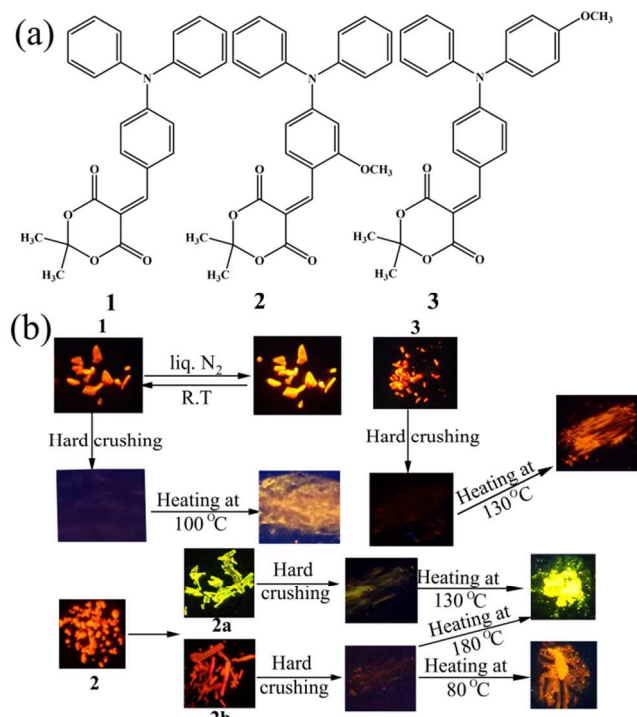
Bright red crystalline powder. Yield: 82%. M. p.: 150 °C, <sup>1</sup>H-NMR (300 MHz, CDCl<sub>3</sub>) δ 8.29 (s, 1H), 8.09 (d, 2H), 7.39-7.34 (m, 2H), 7.22-7.12 (m, 5H), 6.93-6.86 (m, 4H), 3.83 (s, 3H), 1.77 (s, 6H). <sup>13</sup>C-NMR (75 MHz, CDCl<sub>3</sub>) δ 164.8, 161.0, 158.0, 157.6, 153.8, 145.2, 137.9, 137.8, 129.8, 128.6, 126.4, 125.8, 123.1, 117.2, 115.2, 107.6, 103.7, 55.5, 27.4. C<sub>26</sub>H<sub>23</sub>NO<sub>5</sub> (429.46): calcd. C 72.71, H 5.40, N 3.26; found C 72.66, H 5.62, N 3.32. LCMS (ESI) calcd. [M<sup>+</sup>]: 429.16, found: 429.2.

## Characterization

NMR spectra were measured on a Bruker 300 MHz AVANCE-II. Fluorescence spectra and absolute quantum yield for all compounds in the solid state were recorded using Jasco fluorescence spectrometer-FP-8300 instruments equipped with integrating sphere and calibrated light source. Lifetime measurements were carried out with a Hamamatsu Photonics Quanta-Tau. DSC scans were recorded on TA Instruments DSC Q20 differential scanning calorimeter. Each sample was sealed in a Tzero aluminum pan/lid. Mass spectra were recorded with a Bruker 320-MS triple quadrupole mass spectrometer using direct probe insertion method. Powder X-ray diffraction (PXRD) patterns were measured using a XRD-Bruker D8 Advance XRD with Cu K $\alpha$  radiation ( $\lambda = 1.54050$  Å) at room temperature. Single crystals were coated with paratone-N oil and the diffraction data measured at 100K with synchrotron radiation ( $\lambda = 0.62998$  Å) on a ADSC Quantum-210 detector at 2D SMC with a silicon (111) double crystal monochromator (DCM) at the Pohang Accelerator Laboratory, Korea. CCDC Nos. – 1563481-1563484, 1563486 and 1563487 contain the supplementary crystallographic data for this paper. The HOMO, LUMO and band gap of all structures are studied using B3PW91/6-31+G(d,p) level theory (Gaussian 09 package).

## 3. Results and Discussion

**1-3** compounds were easily synthesized via condensing different triphenylamine aldehyde with meldrum's acid (Scheme 1a, S1). **1-3** did not show any measurable fluorescence in the solution, however, they showed strong fluorescence in the solid state ( $\Phi_f = 14.6-41.8\%$ , Table 1). The weak/non-fluorescence in solution and strong solid state fluorescence indicate the aggregation enhanced emission phenomena (AEE).<sup>24-26</sup> TPA based donor- $\pi$ -acceptor compounds are known to exhibit AEE phenomena.<sup>29-32,67-69</sup> Scheme 1b shows the different stimuli-responsive behavior of **1-3** in the solid state. Subtle change of **1-3** molecular structure resulted tunable fluorescence from yellow to red (Fig. 1a). **1** showed orange fluorescence ( $\lambda_{\text{max}} = 586$  nm) and **3** exhibited red fluorescence



Scheme 1. molecular structure (a) and different stimuli responsive fluorescence (b).  $\lambda_{\text{exc}} = 365 \text{ nm}$ .

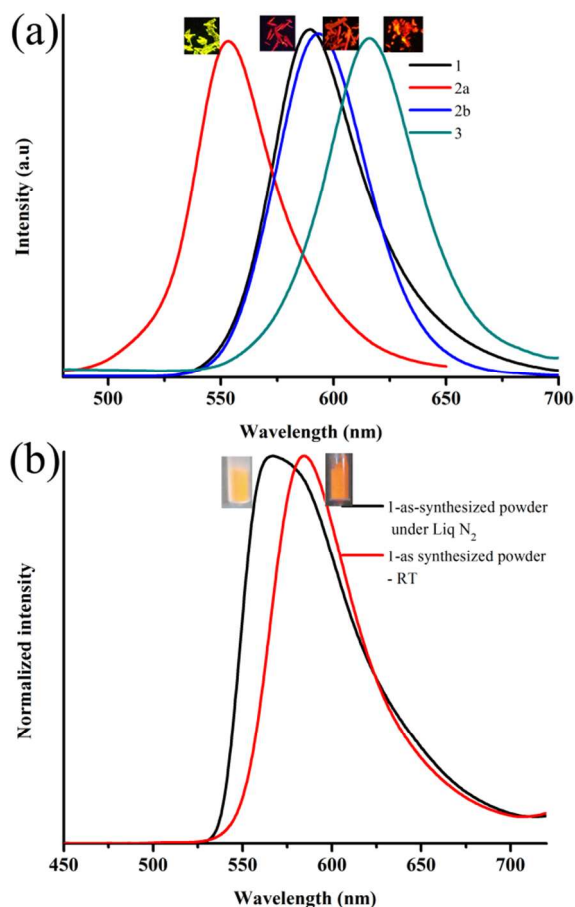


Fig. 1. tunable fluorescence via subtle structural change and (b) TFC of **1**.  $\lambda_{\text{exc}} = 365 \text{ nm}$  (for digital images) and  $370 \text{ nm}$  (for spectra).

Table 1. Fluorescence data of 1-3.

	1	2a	2b	3
Crystals, $\lambda_{\text{max}}$ (nm)	586	553	610	616
$\Phi_f$ (%)	41.8	21.0	15.6	14.6
Hard crushed powders, $\lambda_{\text{max}}$ (nm)	586	553	577	604
$\Phi_f$ (%)	7.6	4.6	3.1	5.7
Heated samples, $\lambda_{\text{max}}$ (nm)	560	553	610 (80 °C) 548 (180 °C)	590
$\Phi_f$ (%)	29.9	13.5	6.5 (80 °C) 13.5 (180 °C)	14.9

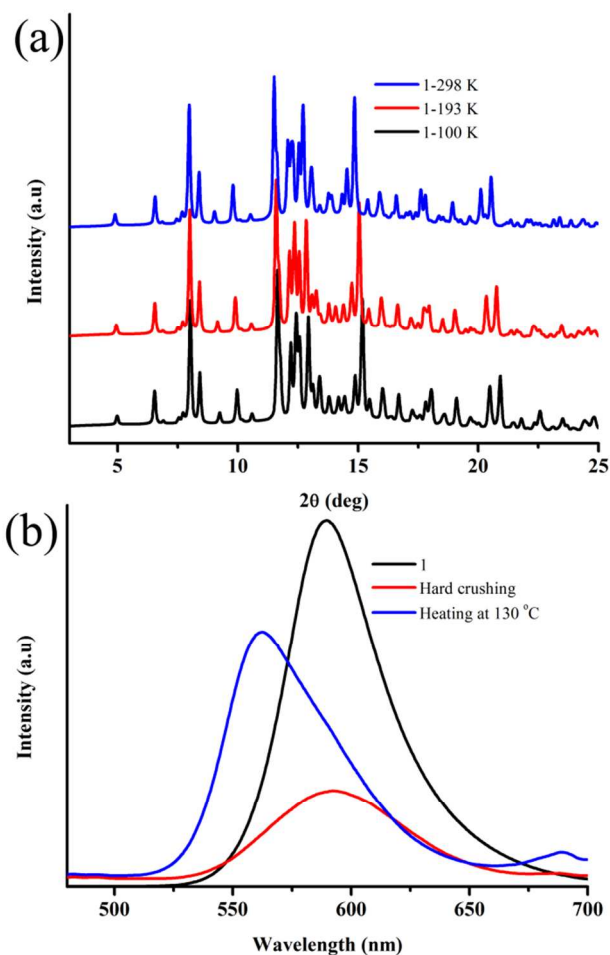


Fig. 2. PXRD pattern of **1** at different temperature and (b) MFC of **1**.  $\lambda_{\text{exc}} = 365 \text{ nm}$  (for digital images) and  $370 \text{ nm}$  (for spectra).

in the solid state ( $\lambda_{\text{max}} = 616 \text{ nm}$ ). The as-synthesized powder of **2** showed red fluorescence and spectra showed peak at  $610 \text{ nm}$  and a small hump at  $548 \text{ nm}$  (Fig. S1a). However, crystallization of **2** produced two concomitant polymorphs (**2a** and **2b**) that exhibited yellow ( $\lambda_{\text{max}} = 553 \text{ nm}$ ) and red fluores-

cence ( $\lambda_{\max} = 610$  nm, Fig. S1b). Interestingly, orange fluorescence of as-synthesized powder as well as crystals of **1** showed blue shift of fluorescence  $\lambda_{\max}$  from 586 to 558 nm upon immersing in liq.  $N_2$  (Fig. 1b, S2). The fluorescence was reversed to initial state upon removing from liq.  $N_2$  within few minutes. PXRD analysis of **1** measured at 298, 193 and 100 K showed small differences in the peak position upon reducing to low temperature (Fig. 2a). However, DSC heating and cooling cycle studies did not show any phase transition except melting at 152 °C (Fig. S3). Due to the instrument limitation, we were able to record DSC up to -80 °C whereas **1** showed color change only when immersed in liq.  $N_2$ . Hence **1** might be having phase transition below -80 °C. Apart from reversible TFC, **1** also showed usual MFC observed for twisted non-planar TPA derivatives. Hard crushing of **1** exhibited strong reduction of fluorescence intensity without shifting  $\lambda_{\max}$  (Fig. 2b, Table 1). The fluorescence was recovered while heating at 130 °C ( $\Phi_f = 29.9\%$ ). Heated solids showed blue shifted fluorescence  $\lambda_{\max}$  that could be attributed to disruption of long range molecular ordering in the solid state.<sup>71-74</sup> PXRD studies of **1** indicated that strong crushing converted crystalline materials to partial amorphous and crystalline phase was recovered by heating (Fig. S4). The PXRD patterns of heated sample matched with initial sample and suggest that there is no

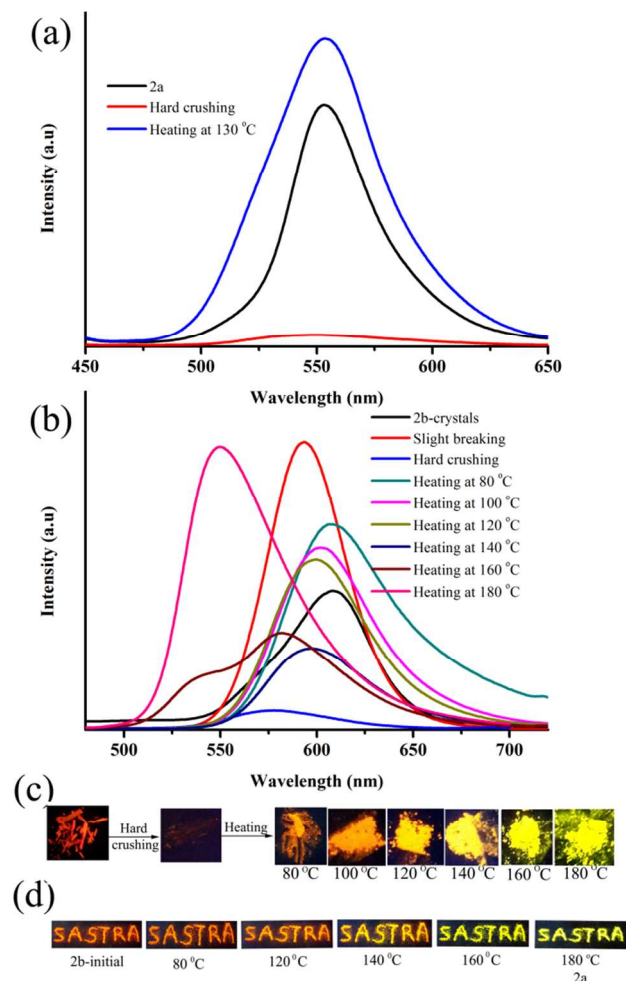


Fig. 3. (a) **2a** MFC, (b) MFC of **2b** with different temperature heating, (c) digital images of fluorescence change with pressure and temperature and (d) topochemical conversion of -2b.  $\lambda_{\text{exc}} = 365$  nm (for digital images) and 370 nm (for spectra).

structural change. Hence MFC of **1** was attributed to the reversible switching of crystalline to partial amorphous and vice versa.

**2** crystals grown from  $CH_2Cl_2$ -hexane mixture showed two different fluorescence color (Fig. S1b), yellow (**2a**, Table 1) and red (**2b**, Table 1). **2a** and **2b** crystals were separated by hand. In contrast to **1**, both yellow and red crystals of **2** did not show any fluorescence change while immersing in liq.  $N_2$ . However, both **2a** and **2b** showed MFC (Fig. 3). Hard crushing of **2a** showed substantial reduction of fluorescence intensity without altering fluorescence  $\lambda_{\max}$  (Fig. 3a, Table 1). The fluorescence was recovered by heating the crushed solids at 130 °C (Table 1). Slight breaking of **2b** crystals showed enhancement of fluorescence intensity with slight blue shift of  $\lambda_{\max}$  (600 nm) that might be attributed to defects generation on the crystals (Fig. 3b).<sup>71-74</sup> Similar to **2a**, hard crushing of **2b** also showed strong reduction of fluorescence intensity with further blue shift of  $\lambda_{\max}$  from 600 to 577 nm (Fig. 3b, Table 1). Interestingly, heating of crushed **2b** solids at different temperature displayed different fluorescence turn-on (Fig. 3b,c). Heating crushed powder at 80 °C exhibited turn-on fluorescence at 610 nm (Table 1). However, further increase of heating temperature (100-140 °C) leads to slight reduction of fluorescence intensity with gradual blue shift of fluorescence. **2b** crushed powder heated at 160 °C showed two fluorescence peaks, 540 and 580 nm. The fluorescence of  $\lambda_{\max}$  was completely shifted to 548 nm with good enhancement of intensity by heating at 180 °C (Table 1). Without crushing, direct heating of **2b** crystals also showed complete conversion of fluorescence from red to yellow at 180 °C (Fig. S5). The

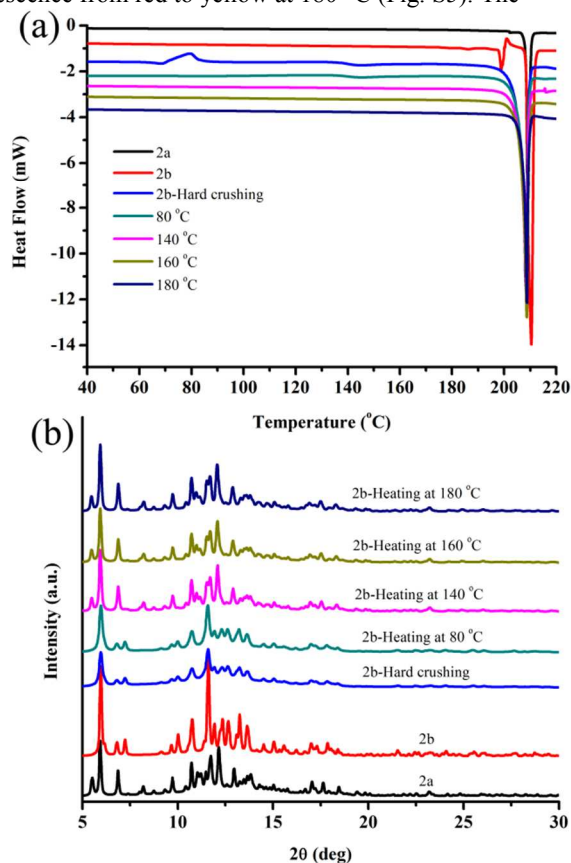


Fig. 4. **2b** DSC (a) and PXRD pattern (b) at different temperature.

topochemical conversion of **2b** has been demonstrated in a pattern using hard crushed powder that showed complete conversion of red fluorescence to yellow upon increasing heating temperature (Fig. 3d). However, heating of **2a** crystals did not show any significant change of fluorescence. DSC studies of **2a** crystals did not show any phase transition before melting and suggest there is no phase or structural transformation (Fig. 4a). However, **2b** crystals exhibited clear phase transition around 190 °C before melting at 210 °C (Fig. 4a). This supports the topochemical transformation of **2b** to **2a**. Hard crushed solids of **2b** exhibited two phase transition, one at 80 and another at 140 °C. The first phase transition for converting amorphous to crystalline form of **2b** and second phase transition is corresponds to topochemical conversion. Hard crushed 80 °C heated **2b** powders showed phase transition at 140 °C corresponds to topochemical conversion. On the other hand, hard crushed, higher temperature (140, 160 and 180 °C) heated powders did not show any phase transition and indicates completion of structural transformation. PXRD studies revealed different diffraction patterns for **2a** and **2b** polymorphs (Fig. 4b). Hard crushing of **2b** leads to the decrease of peak intensity significantly and indicates the formation of partial amorphous solids. The PXRD peaks obtained for the crushed solids matched with **2b** initial pattern. Heating of crushed solids at 80 °C increased the peak intensity without changing the pattern that suggests the improvement of crystallinity. In contrast, the crushed solids heated at 140 °C revealed complete change of peaks position which matched with **2a** rather than **2b**. Higher temperature heating of crushed solids only increased the crystallinity. Thus the first phase transition (80 °C) of **2b** crushed solids was due to conversion of partial amorphous to crystalline whereas second phase transition (140 °C) could be attributed for structural conversion.

**3** showed red fluorescence with relatively weak intensity (Table 1, Fig. S6a) compared to **1** and **2**. On the other hand, **3** did not show reversible TFC or polymorphism rather it showed only usual mechanical shear and heating induced off-on fluorescence switching. Hard crushing of **3** showed strong reduction of fluorescence intensity with small blue shift of fluorescence (Table 1). Heating of hard crushed solids at 130 °C strongly enhanced fluorescence intensity (Table 1). DSC studies clearly revealed a phase transition between 80 and 90 °C (Fig. S6b). PXRD studies suggested the conversion of crystalline to amorphous/partial amorphous state upon hard crushing and amorphous to crystalline state while heating (Fig. S6c). Thus subtle structural change from simple TPA to methoxy substituted TPA significantly influenced on the stimuli-responsive properties of the resulting materials. The fluorescence lifetime measurements revealed bi-exponential decay for **1**, **2b** and **3** whereas **2a** exhibited tri-exponential decay (Fig. S7). The short lifetime (4.10 and 9.37 ns (**1**), 1.28, 7.03, 19.92 ns (**2a**), 4.02 and 8.46 ns (**2b**), 2.98 and 5.85 ns (**3**)) indicates that all compounds shows only fluorescence.

To understand the tunable fluorescence and stimuli-responsive behavior of **1-3**, detailed crystal structure analysis were performed. Single crystal of **1** was grown from slow evaporation of DCM-hexane. **1** structural analysis was performed at 298, 193 and 100 K to gain insight on the reversible TFC. Single crystal of **1** also exhibited clear color change upon cooling from 298 to 100 K (Fig. S8). At all three temperatures, **1** showed similar dimer formation with opposite molecular orientation via C-H...O interactions and interlinking of

dimers via C-H... $\pi$  interactions (Fig. 5a, S9). The molecular packing in the crystal lattice also did not show significant differences (Fig. S10). However, comparison of molecular conformation revealed slight twisting differences in the triphenylamine at different temperature (Fig. 5b, S11, Table S1). The acceptor (meldrum's acid) also showed change of twisting with temperature. The torsional angle ( $\tau$ ) of TPA and meldrum's acid decreased from 4.61 at 298K to 3.78 at 100K (Table S1). The decrease of molecular twist at low temperature might lead to closer packing of the oppositely oriented molecules and increase of optical band gap. It is noted that C-H...O intermolecular distances of **1** was decreased from 3.219 to 3.195 Å with decreasing temperature from 298 to 100K (Fig. 5a, S9) The molecular conformational and packing change induced optical band gap modulation and solid state fluorescence tuning of **1** was further supported by DFT calculations (Fig. 6, Table 2). Single crystal structure of **1** was used for the calculations. **1** structure revealed gradual increase of optical band gap with decreasing temperature. **1** at 298 K exhibited lowest band gap of 3.205 eV whereas it showed 3.24 eV at 100 K. Thus slight conformational change with decreasing temperature leads to increase of band gap. **2** produced yellow

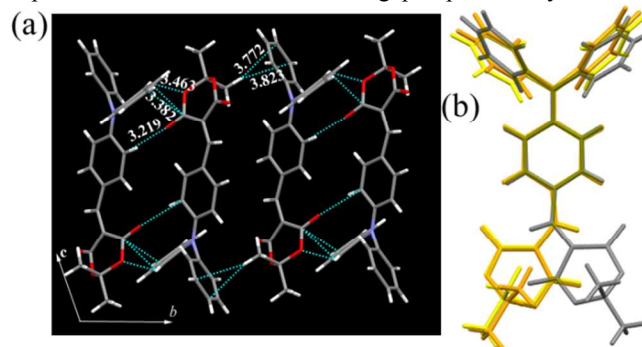


Fig. 5. (a) Dimer and linking of dimers in the crystal lattice of **1** (298 K) and (b) superimposed molecular conformation of **1** displayed in the crystal lattice at different temperature. **1**-298K (grey), 193K (yellow) and 100K (orange). C (grey), N (blue), O (red), H (white); H-bonds (broken line).  $d_{D...A}$  distances are marked (Å).

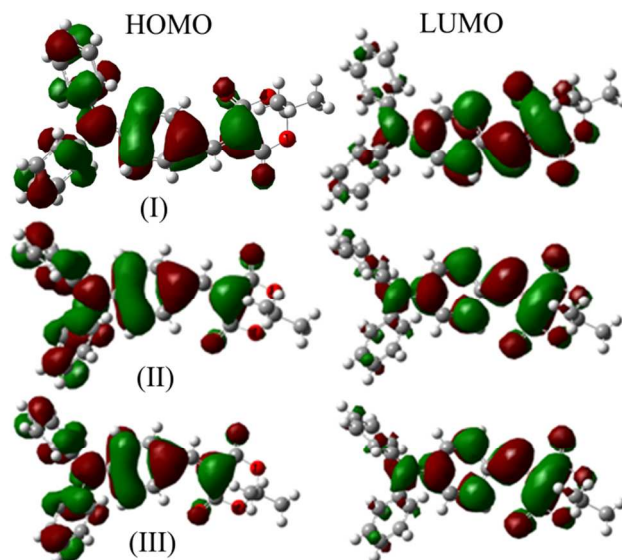


Figure 6. Molecular orbital plots of the HOMOs and LUMOs of **1** at (I) 298K, (II) 193K and (III) 100K.

**Table 2. Computational HOMO-LUMO band gap value of 1-3.**

Compound	HOMO (eV)	LUMO (eV)	Band gap (eV)
<b>1</b> (298 K)	-5.754	-2.549	3.205
<b>1</b> (193 K)	-5.752	-2.532	3.220
<b>1</b> (100 K)	-5.75	-2.51	3.24
<b>2a</b>	-5.721	-2.221	3.500
<b>2b</b>	-5.633	-2.451	3.182
<b>3</b>	-5.635	-2.448	3.187

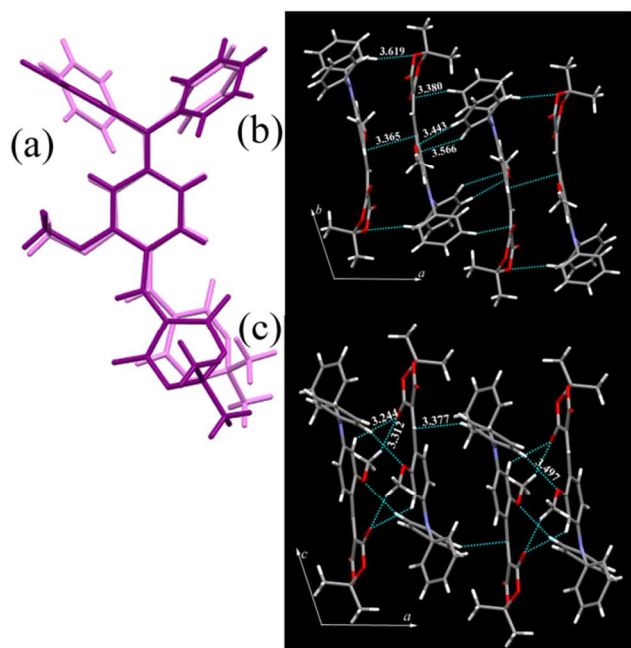


Fig. 7. (a) Superimposed molecular conformation of **2** in polymorphs (**2a** (purple) and **2b** (pink)) and dimer and linking of dimers in the crystal lattice of (b) -**2a** and (c) -**2b**. C (grey), N (blue), O (red), H (white); H-bonds (broken line).  $d_{D...A}$  distances are marked (Å).

(**2a**) and red (**2b**) polymorphs by slow evaporation of  $\text{CH}_2\text{Cl}_2$ - $\text{CH}_3\text{OH}$ . Structural analysis revealed different molecular conformation and crystal packing in the crystal lattice of **2a** and **2b** (Fig. 7a, S12, Table S1). **2a** showed dimer formation with opposite molecular orientation through  $\pi$ - $\pi$  interactions (Fig. 7b). The C-H... $\pi$  and C-H...O interactions further interlink the dimers along *a*-axis. Dimers were also linked along *c*-axis via C-H...O interactions between methoxy methyl hydrogen and meldrum's acid carbonyl oxygen (Fig. S13). **2b** showed dimer formation via C-H...O intermolecular interactions between carbonyl oxygen and phenyl and methoxy methyl hydrogen (Fig. 7c). Further C-H...O interactions interlink the dimers along *b*-axis (Fig. S14). Triphenylamine in the crystal lattice of **2b** exhibited highest twist compared to the crystal lattice of **2b**. However, meldrum's acid was strongly twisted in **2b** ( $\tau = 23.56$ ) compared to -**2a** ( $\tau = 7.26$ ). Compu-

tational studies of **2** polymorphic structures clearly demonstrated band gap differences (Fig. S15, Table S1). The higher triphenylamine twisting and lower acceptor twisting lead to higher band gap (3.50 eV) for **2a** compared to **2b** band gap of 3.182 eV. The stabilization and free energies calculation suggests that **2b** structure is more stable than **2a** structure by -3.3 kcal/mol. However, stability of **2a** was increased from room temperature to 453 K by -26.5 kcal/mol. This might be the reason for **2b** exhibiting topochemical conversion while heating at 140 °C (Fig. 3b,c,S5). The crystal lattice of **3** (grown from  $\text{CH}_3\text{OH}$ ) also revealed  $\pi$ - $\pi$  interactions induced opposite molecular oriented dimer and interlinking of dimer by C-H... $\pi$  interactions (Fig. 8a, S16). Theoretical calculation showed band gap of 3.187 eV (Fig. S17). Comparison of crystal structures showed clear conformational changes by  $\text{OCH}_3$  substitution and polymorphism (Fig. 8b,S18). The modulation of conformation and packing lead to tunable fluorescence that was further supported by theoretical calculation. Further, the structural and solid state fluorescence comparison indicates that increase of acceptor twist (meldrum's acid) lead to red shift of fluorescence whereas smaller twist showed blue shifted fluorescence.

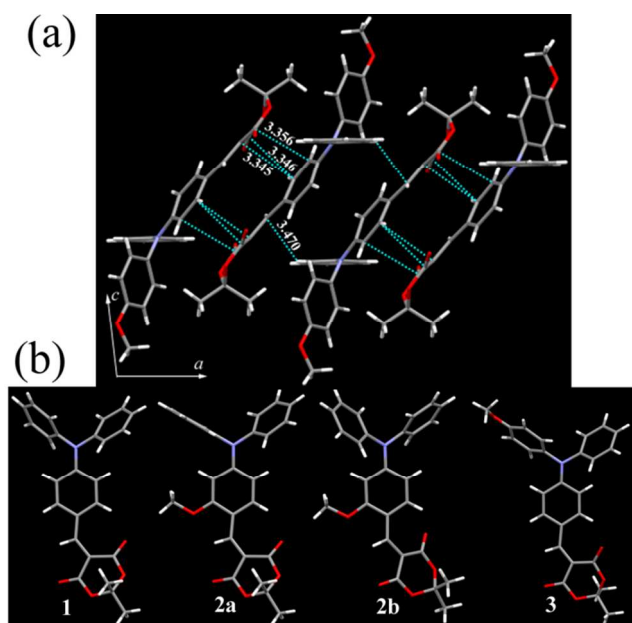


Fig. 8. (a) Dimer and linking of dimers in the crystal lattice of **3** and (b) comparison of molecular conformation in the crystal lattice of **1-3**. C (grey), N (blue), O (red), H (white); H-bonds (broken line).  $d_{D...A}$  distances are marked (Å).

#### 4. Conclusion

In conclusion, subtle structural change controlled tunable and stimuli responsive fluorescence including rare polymorph controlled MFC when heated at different temperature has been demonstrated. **1-3** showed strong tunable fluorescence in the solid state (552 to 616 nm,  $\Phi_f = 14.6$ – $41.8$  %). **1** showed reversible TFC at liq.  $\text{N}_2$  and room temperature. Crystal structural analysis indicated conformational change of TPA upon reducing temperature and PXRD pattern revealed slight peak position change. Computational studies supported conformation induced optical band gap modulation. **2b** showed rare two different MFC when heated at 80 and 180 °C and topochemical conversion. PXRD studies confirmed conversion of partial amorphous to crystalline while heating at 80 °C where-

as conversion of **2b** to **2a** at higher temperature heating. DSC studies showed two phase transition (80 and 140 °C) for strongly crushed **2b**. In contrast, **2a** and **3** showed usual MFC via reversible phase transformation. Thus the present studies suggests that conformationally flexible TPA especially with OCH<sub>3</sub> substituent at *ortho* position to acceptor could be a potential building unit to develop polymorphic, topochemical as well as multi-stimuli responsive smart fluorescent materials.

Supporting Information: Synthesis scheme, NMR spectra, crystallographic table, fluorescence spectra, crystal structure, HOMO-LUMO molecular diagram, lifetime, DSC and PXRD studies.

### Corresponding Author

\*<sup>a)</sup>Savarimuthu Philip Anthony, Department of Chemistry, School of Chemical & Biotechnology, SASTRA Deemed University, Thanjavur-613401, Tamil Nadu, India.

(philip@biotech.sastra.edu)

\*<sup>d)</sup>Beamline Department, Pohang Accelerator Laboratory, 80 Jigokro-127beongil, Nam-gu, Pohang, Gyeongbuk, Korea. (dmoon@postech.ac.kr)

### ACKNOWLEDGMENT

Financial support from the Science and Engineering Research Board (SERB), New Delhi, India (SERB No. EMR/2015/00-1891) is acknowledged with gratitude. "X-ray crystallography at the PLS-II 2D-SMC beamline was supported in part by MSIP and POSTECH. DSC studies were supported by Basic Science Research Program through the National Research Foundation of Korea (NRF) funded by the Ministry of Education, Science and Technology (NRF-2017R1C1B2003111).

### REFERENCES

- Zuccherro, A. J.; McGrier, P. L.; Bunz, U. H. F. Cross-Conjugated Cruciform Fluorophores. *Acc. Chem. Res.* **2010**, *43*, 397-408.
- Xu, S. D.; Yuan, Y. Y.; Cai, X. L.; Zhang, C. J.; Hu, F.; Liang, J.; Zhang, G. X.; Zhang, D. Q.; Liu, B. Tuning the singlet-triplet energy gap: a unique approach to efficient photosensitizers with aggregation-induced emission (AIE) characteristics. *Chem. Sci.* **2015**, *6*, 5824-5830.
- Zhu, L.; Tran, H.; Beyer, F. L.; Walck, S. D.; Li, X.; Ågren, H.; Killops, K. L.; Campos, L. M. J. Engineering Topochemical Polymerizations Using Block Copolymer Templates. *J. Am. Chem. Soc.* **2014**, *136*, 13381-13387.
- Shao, A. D.; Xie, Y. S.; Zhu, S. J.; Guo, Z. Q.; Zhu, S. Q.; Guo, J.; Shi, P.; James, T. D.; Tian, H.; Zhu, W. H. Far-Red and Near-IR AIE-Active Fluorescent Organic Nanoprobes with Enhanced Tumor-Targeting Efficacy: Shape-Specific Effects. *Angew. Chem. Int. Ed.* **2015**, *54*, 7275-7280.
- Ding, Y. B.; Tang, Y. Y.; Zhu, W. H.; Xie, Y. S. Fluorescent and colorimetric ion probes based on conjugated oligopyrroles. *Chem. Soc. Rev.* **2015**, *44*, 1101-1112.
- Ding, Y. B.; Zhu, W. H.; Xie, Y. S. *Chem. Rev.* **2016**, *116*, 4512.
- Zhang, X.; Rehm, S.; Safont-Sempere M. M.; Würthner, F. Vesicular perylene dye nanocapsules as supramolecular fluorescent pH sensor systems. *Nat. Chem.* **2009**, *1*, 623-629.
- Sagara, Y.; Kato, T. Mechanically induced luminescence changes in molecular assemblies. *Nat. Chem.* **2009**, *1*, 605-610.
- Yang, X.; Huang, H.; Pan, B.; Aldred, M. P.; Zhuang, S.; Wang, L.; Chen J.; and Ma, D. G. Modified 4,4',4"-Tri(N-carbazolyl) triphenylamine as a Versatile Bipolar Host for Highly Efficient Blue, Orange, and White Organic Light-Emitting Diodes. *J. Phys. Chem. C* **2012**, *116*, 15041-15044.
- Sagara, Y.; Yamane, S.; Mitani, M.; Weder, C.; Kato, T. Mechano-responsive Luminescent Molecular Assemblies: An Emerging Class of Materials. *Adv. Mater.* **2016**, *28*, 1073-1095.
- Shi, H.; Ma, X.; Zhao, Q.; Liu, B.; Qu, Q.; An, Z.; Zhao Y.; Huang, W. Ultrasmall Phosphorescent Polymer Dots for Ratiometric Oxygen Sensing and Photodynamic Cancer Therapy. *Adv. Funct. Mater.* **2014**, *24*, 4823-4830.
- Feng, H.-T.; Xiong, J.-B.; Zheng, Y.-S.; Pan, B.; Zhang, C.; Wang L.; Xie, Y. Multicolor Emissions by the Synergism of In-

tra/Intermolecular Slipped  $\pi$ - $\pi$  Stackings of Tetraphenylethylene-DIBODIPY Conjugate. *Chem. Mater.* **2015**, *27*, 7812-7819.

(13) Srujana, P.; Radhakrishnan, T. P. Extensively Reversible Thermal Transformations of a Bistable, Fluorescence-Switchable Molecular Solid: Entry into Functional Molecular Phase-Change Materials. *Angew. Chem. Int. Ed.* **2015**, *54*, 7270-7274.

(14) Anthony, S. P. Organic Solid-State Fluorescence: Strategies for Generating Switchable and Tunable Fluorescent Materials. *ChemPlusChem* **2012**, *77*, 518-531.

(15) Qi, Q.; Qian, J.; Tan, X.; Zhang, J.; Wang, L.; Xu, B.; Zou, B.; Tian, W. Remarkable Turn-On and Color-Tuned Piezochromic Luminescence: Mechanically Switching Intramolecular Charge Transfer in Molecular Crystals. *Adv. Funct. Mater.* **2015**, *25*, 4005-4010.

(16) Chi, Z.; Zhang, X.; Xu, B.; Zhou, X.; Ma, C.; Zhang, Y.; Liu, S.; Xu, J. Recent advances in organic mechanofluorochromic materials. *Chem. Soc. Rev.* **2012**, *41*, 3878-3896.

(17) Sagara, Y.; Mutai, T.; Yoshikawa, I.; Araki, K. J. Material Design for Piezochromic Luminescence: Hydrogen-Bond-Directed Assemblies of a Pyrene Derivative. *J. Am. Chem. Soc.* **2007**, *129*, 1520-1521.

(18) Zhang, J.; Xu, W.; Sheng, P.; Zhao, G.; Zhu, D. Organic Donor-Acceptor Complexes as Novel Organic Semiconductor. *Acc. Chem. Res.* **2017**, *50*, 1654-1662.

(19) Mannix, A.; Zhou, X.; Kiraly, B.; Wood, J.; Alducin, D.; Myers, B.; Liu, X.; Fisher, B.; Santiago, U.; Guest, J.; Yacamán, M.; Ponce, A.; Oganov, A.; Hersam, M.; Guisinger, N. Synthesis of borophenes: Anisotropic, two-dimensional boron polymorphs. *Science* **2015**, *350*, 1513-1516.

(20) Anthony S. P.; and Draper, S. M. Nano/microstructure fabrication of functional organic material: Polymorphic structure and tunable luminescence. *J. Phys. Chem. C* **2010**, *114*, 11708-11716.

(21) Anthony, S. P.; Varughese S.; and Draper S. M. Switching and tuning organic solid-state luminescence via a supramolecular approach. *Chem. Commun.* **2009**, 7500-7502.

(22) Song, Q.; Wang, Y.; Hu, C.; Zhang, Y.; Sun, J.; Wang K.; Zhang, C. Effect of stacking mode on the mechanofluorochromic properties of 3-aryl-2-cyano acrylamide derivatives. *New J. Chem.* **2015**, *39*, 659-663.

(23) Wu, H.; Hang, C.; Li, X.; Yin, L.; Zhu, M.; Zhang, J.; Zhou, Y.; Ågren, H.; Zhang Q.; Zhu, L. Molecular Stacking Dependent Phosphorescence-Fluorescence Dual Emission on Single Luminophore for Self-Recoverable Mechanoconversion of Multicolor Luminescence. *Chem. Commun.* **2017**, *53*, 2661-2664.

(24) Fang, M.; Yang, J.; Liao, Q.; Gong, Y.; Xie, Z.; Chi, Z.; Peng, Q.; Li Q.; Li, Z. J. Triphenylamine derivatives: different molecular packing and the corresponding mechanoluminescent or mechanochromism property. *J. Mater. Chem. C* **2017**, *5*, 9879-9885.

(25) Yagai, S.; Okamura, S.; Nakano, Y.; Yamauchi, M.; Kishikawa, K.; Karatsu, T.; Kitamura, A.; Ueno, A.; Kuzuhara, D.; Yamada, H.; Seki, T.; Ito, H. Design amphiphilic dipolar  $\pi$ -systems for stimuli-responsive luminescent materials using metastable states. *Nat Commun* **2014**, *5*, 4013.

(26) Dong, Y. Q.; Lam, J. W. Y.; Qin, A. J.; Sun, J. X.; Liu, J. Z.; Li, Z.; Sun, J. Z.; Sung, H. H. Y.; Williams, I. D.; Kwok H. S.; Tang, B. Z. Aggregation-induced and crystallization-enhanced emissions of 1,2-diphenyl-3,4-bis(diphenylmethylene)-1-cyclobutene. *Chem. Commun.* **2007**, 3255-3257.

(27) Kundu, A.; Hariharan, P.S.; Prabakaran, K.; Moon, D.; Anthony, S. P. Stimuli responsive reversible high contrast off-on fluorescence switching of simple aryl-ether amine based aggregation-induced enhanced emission materials. *RSC Advances* **2015**, *5*, 98618- 98625

(28) Hariharan, P. S.; Venkataramanan, N. S.; Moon, D.; Anthony, S. P. Self-Reversible Mechanochromism and Thermochromism of a Triphenylamine-Based Molecule: Tunable Fluorescence and Nanofabrication Studies. *J. Phys. Chem. C* **2015**, *119*, 9460-9469.

(29) Hariharan, P.S.; Prasad, V.K.; Nandi, S.; Anoop, A.; Moon, D.; Anthony, S. P. Molecular Engineering of Triphenylamine Based Aggregation Enhanced Emissive Fluorophore: Structure-Dependent Mechanochromism and Self-Reversible Fluorescence Switching. *Cryst. Growth Des.* **2017**, *17*, 146-155.

(30) Hariharan, P. S.; Gayathri, P.; Moon, D.; Anthony, S. P. Tunable and Switchable SolidState Fluorescence: Alkyl Chain Length-Dependent Molecular Conformation and Self-Reversible Thermochromism. *ChemistrySelect* **2017**, *2*, 7799-7807.

(31) Hariharan, P. S.; Mothi, E. M.; Moon, D.; Anthony, S. P. Halochromic Isoquinoline with Mechanochromic Triphenylamine: Smart Fluorescent Material for Rewritable and Self-Erasable Fluorescent Platform. *ACS Appl. Mater. Interfaces* **2016**, *8*, 33034-33042.

(32) Hariharan, P. S.; Moon, D.; Anthony, S. P. Reversible fluorescence switching and topochemical conversion in an organic AEE mate-

rial: polymorphism, defection and nanofabrication mediated fluorescence tuning. *J. Mater. Chem. C* **2015**, *3*, 8381-8388.

(33) Wang, Y. L.; Liu, W.; Bu, L. Y.; Li, J. F.; Zheng, M.; Zhang, D. T.; Sun, M. X.; Tao, Y.; Xue, S. F.; Yang, W. J. Reversible piezochromic luminescence of 9,10-bis[(N-alkylcarbazol-3-yl) vinyl] anthracenes and the dependence on N-alkyl chain length. *J. Mater. Chem. C* **2013**, *1*, 856-862.

(34) Bu, L. Y.; Sun, M. X.; Zhang, D. T.; Liu, W.; Wang, Y. L.; Zheng, M.; Xue, S. F.; Yang, W. J. Solid-state fluorescence properties and reversible piezochromic luminescence of aggregation-induced emission-active 9,10-bis[(9,9-dialkylfluorene-2-yl) vinyl] anthracenes. *J. Mater. Chem. C* **2013**, *1*, 2028-2035.

(35) Hariharan, P. S.; Moon, D.; Anthony, S. P. Crystallization-induced reversible fluorescence switching of alkyl chain length dependent thermally stable supercooled organic fluorescent liquids. *CrystEngComm* **2017**, *19*, 6489-6497.

(36) Kundu, A.; Karthikeyan, S.; Moon, D.; Anthony, S. P. Self-reversible thermofluorochromism of D-A-D triphenylamine derivatives and the effect of molecular conformation and packing. *CrystEngComm* **2017**, *19*, 6979-6985.

(37) Yuan, M.; Wang, D.; Xue, P.; Wang, W.; Wang, J.C.; Tu, Q.; Liu, Z.; Liu, Y.; Zhang, Y.; Wang, J. Fluorenone Organic Crystals: Two-Color Luminescence Switching and Reversible Phase Transformations between  $\pi$ - $\pi$  Stacking-Directed Packing and Hydrogen Bond-Directed Packing. *Chem. Mater.* **2014**, *26*, 2467-2477.

(38) Varghese S.; Das, S. Role of Molecular Packing in Determining Solid-State Optical Properties of  $\pi$ -Conjugated Materials. *J. Phys. Chem. Lett.* **2011**, *2*, 863-873.

(39) Misra, R.; Jadhav, T.; Dhokale, B.; Mobin, S. M. Reversible mechanochromism and enhanced AIE in tetraphenylethene substituted phenanthroimidazoles. *Chem. Commun.*, **2014**, *50*, 9076-9078.

(40) Jadhav, T.; Dhokale, B.; Misra, R. Effect of cyano group on solid state photophysical behavior of tetraphenylethene substituted benzothiadiazoles. *J. Mater. Chem. C*, **2015**, *3*, 9063-9068.

(41) Jadhav, T.; Dhokale, B.; Mobin, S. M.; Misra, R., Aggregation induced emission and mechanochromism in pyrenoidiazoles. *J. Mater. Chem. C*, **2015**, *3*, 9981-9988.

(42) Ekbote, A.; Jadhav, T.; Misra, R. T-shaped donor-acceptor-donor type tetraphenylethene substituted quinoxaline derivatives: Aggregation induced emission and mechanochromism. *New J. Chem.* **2017**, *41*, 9346-9353.

(43) Sagara, Y.; Lavrenova, A.; Crochet, A.; Simon, Y. C.; Fromm, K. M.; Weder, C. A Thermo- and Mechano-responsive Cyano-Substituted Oligo (p-phenylene vinylene) Derivative with Five Emissive States. *Chem. Eur. J.* **2016**, *22*, 4374-4378.

(44) Sagara, Y.; Kato, T. Brightly Tricolored Mechanochromic Luminescence from a Single-Luminophore Liquid Crystal: Reversible Writing and Erasing of Images. *Angew. Chem. Int. Ed.* **2011**, *50*, 9128-9132.

(45) Martínez-Abadía, M.; Varghese, S.; Giménez, R.; Ros, M. B. Multiresponsive luminescent dicyanodistyrylbenzenes and their photochemistry in solution and in bulk. *J. Mater. Chem. C*, **2016**, *4*, 2886-2893.

(46) Yan, D.; Evans, D. G. Molecular crystalline materials with tunable luminescent properties: from polymorphs to multi-component solids. *mater. Horiz.* **2014**, *1*, 46-57.

(47) Gu, Y.; Wang, K.; Dai, Y.; Xiao, G.; Ma, Y.; Qiao, Y.; Zou, B. Pressure-Induced Emission Enhancement of Carbazole: The Restriction of Intramolecular Vibration. *J. Phys. Chem. Lett.* **2017**, *8*, 4191-4196.

(48) Feng, C.; Wang, K.; Xu, Y.; Liu, L.; Zou, B.; Lu, P. Unique piezochromic fluorescence behavior of organic crystal of carbazole-substituted CNDSB. *Chem. Commun.* **2016**, *52*, 3836-3839.

(49) Mutai, T.; Satou, H.; Araki, K. Reproducible on-off switching of solid-state luminescence by controlling molecular packing through heat-mode interconversion. *Nature materials*, **2005**, *4*, 685-687.

(50) Zhao, Y.; Gao, H.; Fan, Y.; Zhou, T.; Su, Z.; Liu, Y.; Wang, Y. Thermally Induced Reversible Phase Transformations Accompanied by Emission Switching Between Different Colors of Two Aromatic-Amine Compounds. *Adv. Mater.* **2009**, *21*, 3165-3169.

(51) Mutai, T.; Tomoda, H.; Ohkawa, T.; Yabe, Y.; Araki, K. Switching of Polymorph-Dependent ESIPt Luminescence of an Imidazo[1,2-a]pyridine Derivative. *Angew. Chem. Int. Ed.* **2008**, *47*, 9522-9524.

(52) Lavrenova, A.; Diederik Balkenende, W. R.; Sagara, Y.; Schrettl, S.; Simon, C.; Weder, C. Mechano- and Thermo-responsive Photoluminescent Supramolecular Polymer. *J. Am. Chem. Soc.* **2017**, *139*, 4302-4305.

(53) Sagara, Y.; Kubo, K.; Nakamura, T.; Tamaoki, N.; Weder, C. Temperature-Dependent Mechanochromic Behavior of Mechano-responsive Luminescent Compounds. *Chem. Mater.* **2017**, *29*, 1273-1278.

(54) Ito, H.; Muromoto, M.; Kurenuma, S.; Ishizaka, S.; Kitamura, N.; Sato, H.; Seki, T. Mechanical stimulation and solid seeding trigger single-crystal-to-single-crystal molecular domino transformations. *Nat. Commun.* **2013**, *4*, 2009 (1-5).

(55) Wang, K.; Zhang, H.; Chen, S.; Yang, G.; Zhang, J.; Tian, W.; Su, Z.; Wang, Y. Organic Polymorphs: One-Compound-Based Crystals with Molecular-Conformation- and Packing-Dependent Luminescent Properties. *Adv. Mat.* **2014**, *26*, 6168-6173.

(56) Yang, J.; Ren, Z.; Chen, B.; Fang, M.; Zhao, Z.; Tang, B. Z.; Qi, P.; Li, Z. Three polymorphs of one luminogen: how the molecular packing affects the RTP and AIE properties. *J. Mater. Chem. C* **2017**, *5*, 9242-9246.

(57) Anthony, S. P. Polymorph-Dependent Solid-State Fluorescence and Selective Metal-Ion-Sensor Properties of 2-(2-Hydroxyphenyl)-4(3H)-quinazolinone. *Chemistry—An Asian J.* **2012**, *7*, 374-379.

(58) Hariharan, P. S.; Mariyatra, M. B.; Mothi, E. M.; Neels, A.; Rossair, G.; Anthony, S. P. Polymorphism and benzene solvent controlled stimuli responsive reversible fluorescence switching in triphenylphosphoniumfluorenylide crystals. *New J. Chem.* **2017**, *41*, 4592-4598.

(59) Zhang, Y.; Song, Q.; Wang, K.; Mao, W.; Cao, F.; Sun, J.; Zhan, L.; Lv, Y.; Ma, Y.; Zou, B.; Zhang, C. Polymorphic crystals and their luminescence switching of triphenylacrylonitrile derivatives upon solvent vapour, mechanical, and thermal stimuli. *J. Mater. Chem. C* **2015**, *3*, 3049-3054.

(60) Botta, C.; Benedini, S.; Carlucci, L.; Forni, A.; Marinotto, D.; Nitti, A.; Pasini, D.; Righetto, S.; Cariati, E. Polymorphism-Dependent Aggregation Induced Emission of a Push-Pull Dye and its Multi-Stimuli Responsive Behavior. *J. Mater. Chem. C* **2013**, *00*, 1-3.

(61) Du, X.; Xu, F.; Yuan, M.; Xue, P.; Zhao, L.; Wang, D.; Wang, W.; Tu, Q.; Chena, S.; Wang, J. Reversible luminescence color switching in the crystal polymorphs of 2,7-bis(20-methyl-[1,10-biphenyl]-4-yl)-fluorenone by thermal and mechanical stimuli. *J. Mater. Chem. C*, **2016**, *4*, 8724-8730.

(62) Lei, Y.; Liu, Y.; Guo, Y.; Chen, J.; Huang, X.; Gao, W.; Qian, L.; Wu, H.; Liu, M.; Cheng, Y. Multi-Stimulus-Responsive Fluorescent Properties of Donor- $\pi$ -Acceptor Indene-1,3-dionemethylene-1,4-dihydropyridine Derivatives. *J. Phys. Chem. C* **2015**, *119*, 23138-23148.

(63) Xue, P.; Chen, P.; Jia, J.; Xu, Q.; Sun, J.; Yao, B.; Zhang, Z.; Lu, R. A triphenylamine-based benzoxazole derivative as a high-contrast piezofluorochromic material induced by protonation. *Chem. Commun.* **2014**, *50*, 2569-2571.

(64) Gong, Y.; Tan, Y.; Liu, J.; Lu, P.; Feng, C.; Yuan, W. Z.; Lu, Y.; Sun, J. Z.; He, G.; Zhang, Y. Twisted D-p-A solid emitters: efficient emission and high contrast mechanochromism. *Chem. Commun.* **2013**, *49*, 4009.

(65) Tian, H. N.; Yang, X. C.; Pan, J. X.; Chen, R. K.; Liu, M.; Zhang, Q. Y.; Hagfeldt, A.; Sun, L. C. A Triphenylamine Dye Model for the Study of Intramolecular Energy Transfer and Charge Transfer in Dye-Sensitized Solar Cells. *Adv. Funct. Mat.* **2008**, *18*, 3461-3468.

(66) Mishra, A.; Fischer, M. K. R.; Bäuerle, P. Metal-free organic dyes for dye-sensitized solar cells: from structure: property relationships to design rules. *Angew. Chem. Int. Ed.* **2009**, *48*, 2474-2499.

(67) Zhang, Z.; Wu, Z.; Sun, J.; Yao, B.; Xue, P.; Lu, R.  $\beta$ -Iminoenolate boron complex with terminal triphenylamine exhibiting polymorphism and mechanofluorochromism. *J. Mater. Chem. C* **2016**, *4*, 2854-2861.

(68) Ouyang, M.; Zhan, L.; Lv, X.; Cao, F.; Li, W.; Zhang, Y.; Wang, K.; Zhang, C. Clear piezochromic behaviors of AIE-active organic powders under hydrostatic pressure. *RSC Adv.* **2016**, *6*, 1188-1193.

(69) Cao, Y.; Xi, W.; Wang, L.; Wang, H.; Kong, L.; Zhou, H.; Wu, J.; Tian, Y. Reversible piezofluorochromic nature and mechanism of aggregation-induced emission-active compounds based on simple modification. *RSC Adv.* **2014**, *4*, 24649-24652.

(70) Li, Y.; Xue, L.; Xia, H.; Xu, B.; Wen, S.; Tian, W. Synthesis and properties of polythiophene derivatives containing triphenylamine moiety and their photovoltaic applications. *J. of Polymer Sci: Part A: Polymer Chem.* **2008**, *46*, 3970-3984.

(71) Dong, Y.; Xu, B.; Zhang, J.; Tan, X.; Wang, L.; Chen, J.; Lv, H.; We, S.; Li, B.; Ye, L.; Zou, B.; Tian, W. Piezochromic Luminescence Based on the Molecular Aggregation of 9,10-Bis((E)-2-(pyrid-2-yl) vinyl) anthracene. *Angew. Chem. Int. Ed.* **2012**, *51*, 10782-10785.

(72) Han, T.; Hong, Y.; Xie, N.; Chen, S.; Zhao, N.; Zhao, E.; Lam, J. W. Y.; Sung, H. Y.; Dong, Y.; Tong, B.; Tang, B. Z. Defect-sensitive crystals based on diaminomaleonitrile-functionalized Schiff base with aggregation-enhanced emission. *J. Mater. Chem. C* **2013**, *1*, 7314-7320.

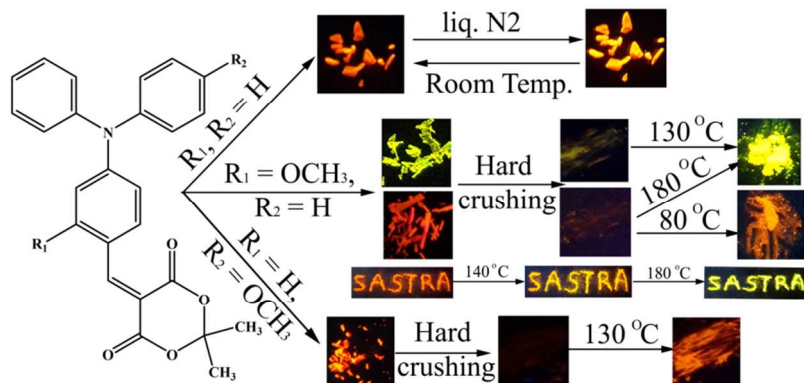
1 (73) Ito, S.; Yamada, T.; Asami, M. Two-Step Mechanochromic Lu-  
2 minescence of N, N'-Bis-Boc-3,3'-di(pyren-1-yl)-2,2'-biindole.  
3 *ChemPlusChem* **2016**, *81*, 1272-1275.

4 (74) Lin, Z.; Mei, X.; Yang, E.; Li, X.; Yao, H.; Wen, G.; Chien, C.-T.;  
5 Chow T. J.; Ling, Q. Polymorphism-dependent fluorescence of bis-  
6 thienylmaleimide with different responses to mechanical crushing and  
7 grinding pressure. *CrystEngComm*. **2014**, *16*, 11018-11026.  
8  
9  
10  
11  
12  
13  
14  
15  
16  
17  
18  
19  
20  
21  
22  
23  
24  
25  
26  
27  
28  
29  
30  
31  
32  
33  
34  
35  
36  
37  
38  
39  
40  
41  
42  
43  
44  
45  
46  
47  
48  
49  
50  
51  
52  
53  
54  
55  
56  
57  
58  
59  
60

“For Table of Contents Use Only”

## Drastic Modulation of Stimuli-Responsive Fluorescence by Subtle Structural Change of Organic Fluorophore and Polymorphism Controlled Mechanofluorochromism

Palamarneri Sivaraman Hariharan,<sup>a</sup> Parthasarathy Gayathri,<sup>a</sup> Anu Kundu,<sup>a</sup> Subramanian Karthikeyan,<sup>b</sup> Yoshimitsu Sagara<sup>c</sup> Dohyun Moon<sup>d\*</sup> Savarimuthu Philip Anthony<sup>a\*</sup>



Aggregation enhanced emissive fluorophore based on triphenylamine exhibited drastic modulation of stimuli-responsive behavior and polymorphism and topochemical conversion induced tunable fluorescence.